HDTMA and TMPA Functionalized Organoclay for Adsorptive Removal of Antimony Sb (III) in Aqueous Solution

Kelechi E Onwuka[1]*, Okechukwu C Atasie[2], Joel C Nwaogwugwu[2], Jude C Igwe[3], Solomon OE Okereke[3] and Williams C Okafor[4]

[1]Research Scholar, Department of Pure and Industrial Chemistry, Abia State University Uturu, Nigeria

[2]Research Scholar, Department of Biochemistry, Abia State University Uturu, Nigeria

[3]Professor, Department of Pure and Industrial Chemistry, Abia State University Uturu, Nigeria

[4]Research Scholar, Bioresource Development Centre, National Biotechnology Development Agency, Nigeria

*Corresponding author: Kelechi E Onwuka, Research Scholar, Department of Pure and Industrial Chemistry, Abia State University Uturu, Nigeria

ARTICLE INFO

Abbreviations: SEM: Scanning Electron Microscopy; XRD: X-Ray Diffraction; FTIR: Fourier Transform Infrared Spec-troscopy

ABSTRACT

The application of hexadecyl trimethyl ammonium and trimethylphenyl ammonium cation functionalized montmorillonite clay has been assessed for adsorptive removal of antimony Sb (III) in aqueous solution. Various adsorption parameters such as contact time, initial adsorbate concentration, pH and temperature have been employed to study Sb (III) adsorption behaviour onto the organoclays. Organ montmorillonite has been initially characterized by scanning electron microscopy (SEM), X-ray diffraction (XRD) and Fourier transform infrared spectroscopy (FTIR). The Langmuir and Freundlich isotherms, as well as pseudo first order, pseudo second order and intraparticle diffusion kinetic models has been exploited in this study to investigate the equilibrium process as well as adsorption mechanism. Results from adsorption studies confirmed 18 and 20 hours as maximum contact time for equilibrium sorption for Mt-TMPA and Mt-HDTMA respectively. Langmuir and pseudo second order kinetic models gave best fit to sorption data. Thermodynamic investigation of the adoption process reveals that the process of Sb (III) adsorption onto the organoclays were feasible and endothermic. About 95.22% and 90.42% removal of Sb (III) was achieved for Mt-HDTMA and Mt-TMPA respectively by reapplication of regenerated spent organoclays for Sb (III) removal within 24 hours contact time. Result from this study substantiates the efficacy of organoclays for effective removal of antimony in aqueous medium.

Keywords: Organoclays; Antimony Sb (III); Adsorption Kinetics; Adsorption Isotherm; Thermodynamics; Montmorillonite

Introduction

Most heavy metal ions especially Sb (III) displays high level of carcinogenicity, as well as toxicity at relatively low concentrations. Antimony has been widely used in lead alloys, battery grids, bearing metal, cable sheathing, plumber's solder, pewter, ammunition, sheet, and pipe [1]. Among the most vital application of antimony in non-metal products are textiles, paints and lacquers, rubber compounds, ceramic enamels, glass and pottery abrasives phosphorus (a

Beryllium replacement), and certain types of matches (SbCl3) [1-3]. US EPA and EU have established 6 and 10 $\mu gL-1$, respectively, of maximum permissible Sb concentrations in drinking water [4,5]. In natural water, Sb mainly exists in the inorganic forms of Sb (III) and Sb(V) [6]. Antimony (III) is reported to be 10 times more toxic than Sb(V) [7-10]. When redox speciation determinations are carried out, numerous studies report the dominance of Sb(V) under oxic conditions. However, the presence of significant proportions of Sb (III) is sometimes detected [6]. The analytical techniques more commonly used for the characterisation of aqueous antimony species are hydride generation methods coupled with AAS, AES, and MS detection systems [1].

Different electrochemical methods have also been used for determination of total antimony in natural water samples. Determination of total antimony by differential pulse anodic stripping voltammetry (DPCSV) has been described by a few authors [11-14]. Niedzielski and Siepak presented a comparative description of different methods of determination of arsenic, antimony, and selenium: spectrophotometric, electroanalytical (voltamperometry), activation analysis, atomic fluorescence, and the methods of inductive or microwave-induced plasma in combination with varieties of detection methods (emission or mass spectrometry) [1,15]. Before now, strategies including coagulation/ precipitation, reverse osmosis and adsorption, have been developed to remove excessive Sb from water [16]. Among these methods, adsorption is still one of the most extensively used. Adsorbent materials, including activated carbon [17], rice husks [3], hydrous oxides of manganese, iron (Fe) and aluminium [18], sand [19], modified home-made thiol cotton fiber [20], chelating porous hollow-fiber membrane [20] and metal oxides like zirconium dioxide, tin dioxide and cerium (IV) oxide [21,22], have been prepared for Sb removal in aqueous solution.

Organoclays are a group of surfactants modified clays with hydrophobic and organophilic surface characteristics that are mostly prepared by intercalating a cationic surfactant between the clay interlayers [23]. Natural clay minerals are not an option for removal of oxyanions and anionic contaminants from the aqueous solutions owing to the presence of negative charges on the surface and interlayers of natural clay minerals occasioned by isomorphic substitution [23]. Hence, intercalation with a cationic surfactant can increase the interlayer spacing and change surface polarity properties of the natural clays [24,25]. The arrangement of organic cations in the interlayers of montmorillonite may form a monolayer, bilayer, paraffin-type monolayer or paraffin-type bilayer depending upon the length of alkyl chain of the organic ion, layer charge of the clay mineral, as well as the way the chains organize themselves in the organoclay [23-25]. The replacement of small exchangeable inorganic cations in the crystalline structure of natural clays with large organic amphiphilic alkylammonium cations such as hexadecyl trimethyl ammonium (HDTMA+) brings about noticeable structural alterations which may consequently affect the diffusion and permeation transport and enhance the uptake capacity of natural clays for anions [26,27].

In addition, through the exchange process of organic cations which can exceed the CEC of the pristine clays, numerous sorption sites for anions are provided [27], which makes the organ minerals promising options for uptake of anionic contaminants from aqueous solutions. Factors such as choice of clay minerals and cationic surfactants as well as the amounts of organic cations chosen might affect the efficacy and adsorption performance of organ minerals [23]. Anjum and Datta [28] studied the adsorptive removal of antimony (III) on modified clays at low concentration range (6μg/L to 100mg/L) and showed that montmorillonites modified with methylpyridinium chloride and cetyl trimethylammonium bromide are efficient adsorbents for the removal of low concentrations of antimonite. Bagherifam, et al. [23] studied the effect of hexadecyl pyridinium chloride modified montmorillonite (HDPy+-M) and hexadecyl pyridinium bromide modified zeolite (HDPy+-Z) on Sb(III) uptake from solutions containing 0.5–2.5 mM antimonite, and their result was quite encouraging.

However, the application of HDTMA and TMPA intercalated montmorillonite for adsorptive removal of Sb (III) in aqueous medium has not been properly investigated. Therefore, this study investigates the application of HDTMA+ (C16) and TMPA+ (C9) intercalated montmorillonite for adsorptive removal of antimony (III) in aqueous solution. Various sorption experimental conditions such as effect of contact time, initial Sb (III) concentration, pH and temperature were applied to study Sb (III) adsorption behaviour onto the organoclays. Adsorption kinetics and isotherms were applied to investigate the mechanism of Sb (III) sorption, and thermodynamics of the adsorption process was also studied to understand the sorption process. The adsorption of Sb (III) by regenerated spent adsorbents were also examined.

Experimental

Materials

The montmorillonite (Mt) clay used in this research was collected from Ropp, Plateau State, situated at Longitude 80E and Latitude 90N, Northern Nigeria, and the clay was beneficiated and pre-modified according to our previous study [29]. The Quaternary akyl ammonium compounds (Surfactants): hexadecyl trimethyl ammonium bromide (HDTMA-Br, C19H42BrN, MW. 364.45) and trimethylphenyl ammonium chloride (TMPA-Cl, C9H14ClN,

MW. 171.5) were procured from Sigma Aldrich Switzerland. Hydroxylamine hydrochloride was procured from Shanghai Aladdin Bio-Chem Technology Co., Ltd. (China). Sodium carbonate was supplied by Sinopharm Chemical Reagent Co., Ltd. (China). All other chemicals used were products of BDH Chemicals, England and all the solutions used were prepared in double distilled water.

Synthesis and Characterization of HDTMA and TMPA Organoclays

Synthesis of organ montmorillonite by HDTMA and TMPA cationic intercalations has been described in detail in a previously published paper [30], characterized for specific surface area by Sear's method [31], cation exchange capacity (CEC) by ammonium acetate procedure [32], IR spectra properties by FTIR spectrophotometer (Buck scientific M530 USA FTIR), basal spacing by X-ray diffraction (Bruker, D8ADVANCE, Germany) using Ni-filtered Cu K$\alpha\alpha$ radiation (1.5406 Å), and morphology by scanning electron microscope (Seron, AIS-2100, Republic of Korea). The values obtained for CEC and specific surface area; Characteristics and physical properties of the unmodified montmorillonite (Mt) and the organo-modified montmorillonite (Mt-HDTMA and Mt-TMPA) were described in detail by our previous work [30].

Batch Adsorption Experiments

The Sb (III)stock solutions (1000 mg·L^{-1}) were prepared by dissolving potassium antimonyl tartrate (2.740 g)in 1000 mL of Distilled water. In adsorption experiments, 0.1 g each of Mt-HDTMA and Mt-TMPA Were separately added into an aqueous solution (400 mL) with initial Sb concentration of 50.00 mg·L^{-1}, and then the mixture was shaken by a thermostatic reciprocating shaker (LHH-250GSP, Bluepard, China) at 300 rpm at 25°C. After reaching adsorption equilibrium, organoclays (Mt-HDTMA and Mt-TMPA) were removed by filtration through 0.35 μm hybrid membranes. The Sb concentrations were determined by atomic absorption spectrometry (contr AA, Jena, Germany) using the high focused short arc xenon lamp of 300W. The wavelength of 217.0 nm was chosen for antimony and acetylene gas of 100 mL·min-1 was applied for flame [33]. The adsorption capacities (qt, qe (mg·g-1)) were calculated based on the following equations:

$$q_t = \frac{(C_0 - C_t)}{m}V \quad \text{(1a)}$$

$$q_e = \frac{(C_0 - C_e)}{m}V \quad \text{(1b)}$$

Where C0 represents initial Sb concentration (mg·L^{-1}), Ct is the Sb concentration (mg·L^{-1}) at time t, Ce is the equilibrium Sb concentration (mg·L^{-1}), v is the solution volume (L) and m is the amount of used adsorbent (g). In the experiments of pH effect, 1.0 mol·L^{-1} of HCl or KOH was used to adjust the solution pH (2, 3, 4,

5, 6, 7, 8 9, and 10). The best candidate for Sb adsorption would be used for other experiments. For the effect of temperature, adsorption experiments were performed at varied temperatures of 25°C, 35°C and 45°C.

Adsorption Kinetics

The kinetic experiments were conducted to investigate the influence of contact time on the organoclays (Mt-HDTMA and Mt-TMPA) adsorption of Sb (III). Organoclays (Mt-HDTMA and Mt-TMPA) of 0.1g was added in 50 mg·L^{-1} Sb solution, and the pH value was adjusted accordingly as above. Intermittently, the mixtures were shaken by a thermostatic reciprocating shaker at 300 rpm, and then sampled at 2, 4, 6, 8, 12, 14, 18, 20 and 24 h for Sb (III) concentrations determination after filtration.

Adsorption Isotherm

Batch isotherm adsorption experiments were conducted with 0.1g organoclays (Mt-HDTMA and Mt-TMPA) within initial Sb (III) concentration range of 10 to 100 mg/L. The pH value was adjusted accordingly as above, and the solution was shaken by a thermostatic reciprocating shaker at 300 rpm at 25°C. After 24 h equilibration, the supernatants were filtered to determine the Sb (III) concentrations.

Regeneration of Sb (III) Saturated Organoclays

The method adopted in our previously published research [34] was applied in the regeneration experiment. This was performed thermally. For this, the organoclays were separately subjected to the adsorption as follows: Initially 0.2 g of the adsorbent was equilibrated in 100 mL of 50 mg/L Sb (III)at the optimum contact time and pH at 25^{0}C. After mixing, the supernatant was centrifuged and analyzed. The saturated clay was then separated and dried at room temperature for 48h. The supposed regenerated organoclays were then placed in an oven at 200^{0}C for 2, 4, 8, 12 and 18 hours. The adsorption experiments were then conducted using the regenerated organoclays.

Results and Discussion

Adsorption Kinetics

Figure 1 represents the effect of contact times in the range of 2 to 24 hrs on the adsorption of Sb (III) by Mt-HDTMA and Mt-TMPA at 250C and initial Sb (III) concentration of 50 mg/L. From Figure 1, rapid adsorption of Sb (III) by the organoclays were observed in the first 14 hrs of the adsorption time, with corresponding adsorption capacities of 39.66and 31.03 mg/g for Mt-HDTMA and Mt-TMPA respectively, and then levelled off as time increased. The adsorption times of 18 and 20 hrs which were little larger than 14 hrswere fixed for the adsorption equilibrium for Mt-TMPA and Mt-HDTMA

respectively. Rapid Sb (III) adsorption by both organoclays suggests the availability of numerous active vacant sites on the organoclay surfaces, followed by a saturated vacant site which accounted for a later slow sorption rate prior to equilibrium sorption.

To further investigate the kinetics of the adsorption process, the experimental data for the adsorption of Sb (III) by the organoclays were modelled into three major kinetic models, namely: pseudo first order, pseudo second order and intra-particle diffusion model (Figures 2-4) using equation (2) - (4) respectively:

$$\log\left(q_e - q_t\right) = \log q_e - \frac{\left(K_1\right)}{2.303}V \quad (2)$$

$$\frac{1}{q_t} = \frac{1}{K_2 q_e^2} + \frac{t}{q_e} \quad (3)$$

$$q_t = K_{id}t^{1/2} + C \quad (4)$$
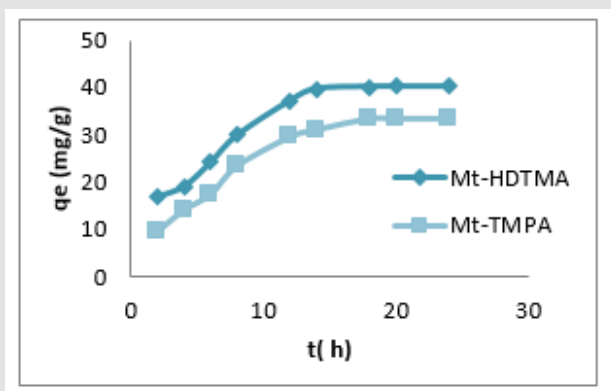
Figure 1: Effect of contact time on the adsorption of Sb (III) by Mt-HDTMA and Mt-TMPA: Initial Sb (III) conc = 50mg/L, Mass = 0.1g, Temp = 25°C, pH=7.
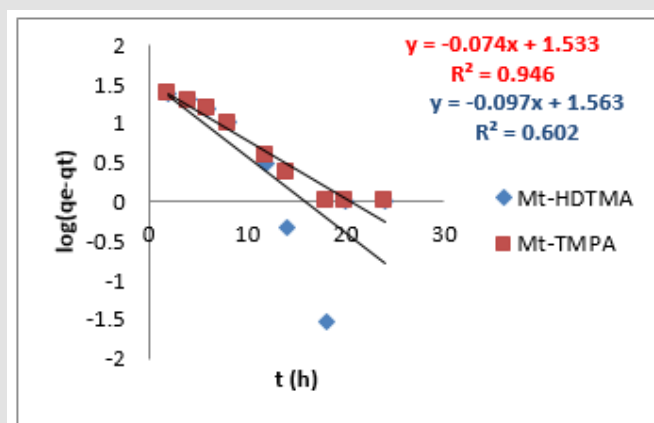
Figure 2: Pseudo first order kinetic plot for Sb (III) adsorption onto Mt-HDTMA and Mt-TMPA.

where q_e (mg/g) is the amount of Sb (III) adsorbed at equilibrium, q_t amount of Sb (III) adsorbed at any given time t (mg/g), k is the rate constant for the pseudo-first-order model, k_2 (g/mg·h) is the rate constant of pseudo-second order, k_{id} (g/mg·h) is the rate of the intraparticle diffusion kinetic model and C is the intraparticle diffusion constant. The obtained values for these kinetic models are summarized in Table 1. From Figures 2-4, it is obvious that three different models in fitting kinetics data for Sb (III) adsorption onto the organoclays were employed. Compared with the pseudo-first-order model, the higher correlation coefficient ($R^2 > 0.98$) revealed that the pseudo-second-order

model was more suitable to describe the adsorption of Sb (III). In addition, the fitted parameters as displayed in Table 1 presented inconsistent $qe_{calculated}$ values of82.5 and 109.23 mg/g (compared to $qe_{experimental}$ values of 40.14 and 33.33 mg/g) for Mt-HDTMA and Mt-TMPA respectively as obtained for the Pseudo first order kinetic model. On the contrary, the $qe_{calculated}$ values for the Pseudo second order kinetic model obtained as 39.97 and 33.62 for Mt-HDTMA and Mt-TMPA respectively, again implies that the pseudo second order kinetic model best fitted the sorption data. This result is in accordance with some previous findings [1,33].
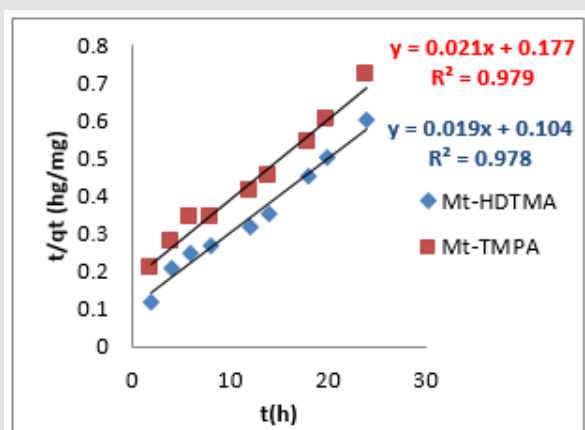
Figure 3: Pseudo second order kinetic plot for Sb (III) adsorption onto Mt-HDTMA and Mt-TMPA.
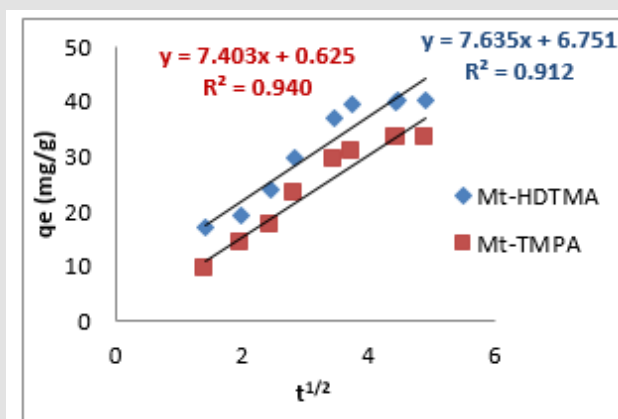
Figure 4: Intraparticle diffusion kinetic plot for Sb (III) adsorption onto Mt-HDTMA and Mt-TMPA.

Table 1: Parameters for the Pseudo first order, Pseudo Second order and intraparticle diffusion kinetic models for the adsorption of Sb(lll) by Mt-HDTMA and Mt-TMPA.

	Pseudo first order			Pseudo Second order				Intraparticle Diffusion		
Adsorbent	$k_1(min)^{-1}$	$q_0(mg/g)$	R^2	$k_2(g/mh.h)$	$q_{0cal}(Mg/g)$	$q_{0exp}(Mg/g)$	R^2	K_{id}	C	R^2
Mt-HDTM	0.062	82.5	0.602	0.022	39.97	40.14	0.978	7.64	0.63	0.912
Mt-TMPA	0.041	109.23	0.946	0.07	33.62	33.33	0.979	7.4	6.75	0.94

Adsorption Isotherms

Adsorption isotherm models are commonly used for describing equilibrium studies and comparing the adsorption capacities of the adsorbents for pollutants [33]. In this study, the adsorption isotherm was modelled with Langmuir and Freundlich isotherm according to equation (5) and (6) respectively:

$$Inq_e = Ink_f + \frac{1}{n} InC_e \quad (5)$$

$$\frac{C_e}{q_e} = \frac{C_e}{Q_m} + \frac{1}{bQ_m} \quad (6)$$

where C_e (mg/L) and q_e (mg/g) are the concentration of adsorbate and the adsorption capacity of the adsorbents at the equilibrium time, respectively, k_f (mg/g) and $1/n$ are the Freundlich constant, b (L/mg) is the Langmuir constant and Q_m (mg/g) is maximum adsorbent capacity. The plots for the Langmuir and Freundlich isotherms are presented in Figures 5 & 6 respectively, and the values of the isotherm parameters obtained by fitting the experimental data to these isotherm models are summarized in Table 2. It is obvious from the higher correlation coefficients that Sb(III) uptake by Mt-HDTMA and Mt-TMPA is better described by the Langmuir isotherm, signifying monolayer adsorption on both organoclays. The maximum adsorption capacity (Q_{max}) for Sb (III) uptake by Mt-HDTMA and Mt- TMPA were calculated to be 43.61

and 38.44 mg/g respectively. Even though the uptake capacity and isotherms of the studied organoclays for Sb(III) removal from aqueous solutions have not been properly reported, the maximum adsorption capacity of both Mt-HDTMA and Mt-TMPA are larger than that of those previously reported by others: bentonite (0.56 mg/g) [35], multi-walled carbon nanotubes (0.32 mg/g) [36], graphene (8.06 mg/g) [37] and polyvinyl alcohol-stabilized granular adsorbent containing nanoscale zero-valent iron (6.99 mg/g) [38]. The results of Freundlich isotherm simulations showed that the 1/n values for Sb (III) uptakes by Mt-HDTMA and Mt-TMPA are less than unity, which based on the statistical theory

of adsorption might be attributed to the heterogeneous surface with minimum interactions between the adsorbed ions based on the statistical theory of adsorption [39], although the isotherms data are best described by the Langmuir model. Furthermore, it is evident (in Figure 7) that the increase in initial Sb (III) concentration resulted to a corresponding increase in the adsorption capacities of the organoclays. This may be due to an increase in driving forces affecting Sb compounds. One of these forces is van der Waal's force that affects active adsorption sites of the adsorbent, which occurs at higher concentrations [29,30,34].
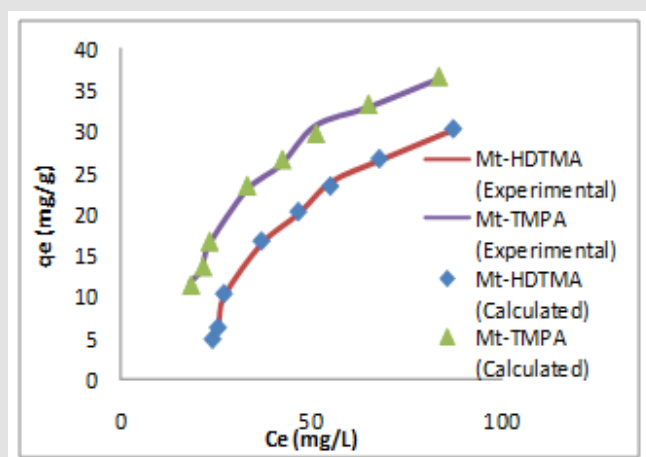
Figure 5: Langmuir isotherm plot for Sb (III) adsorption onto Mt-HDTMA and Mt-TMPA.
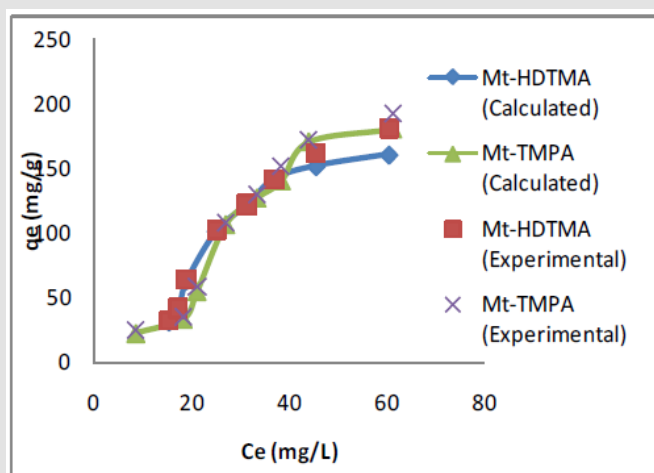
Figure 6: Freundlich isotherm plot for Sb (III) adsorption onto Mt-HDTMA and Mt-TMPA.

Table 2: Isotherm parameters for the adsorption of Sb (lll) by Mt-HDTMA and Mt-TMPA (adsorbent dosage=0.2g).

	Langmuir			Freundlich		
Adsorbent	Qm (mg/g)	b(L/mg)	R^2	K_f(mg/g)	1/n	R^2
Mt-HDTM	43.61	0.004	0.957	12.34	0.55	0.857
Mt-TMPA	38.44	0.32	0.974	40.62	0.071	0.901
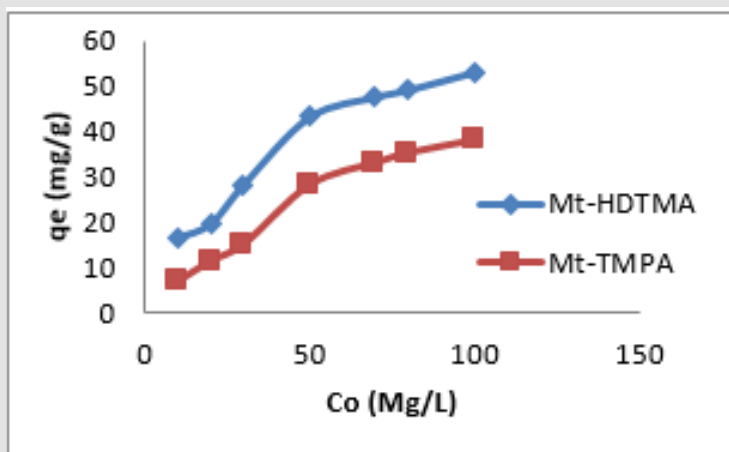
Figure 7: Effect of initial Sb (III) concentration on the adsorption of Sb (III) by Mt-HDTMA and Mt-TMPA: Time = 18 h, mass of adsorbent = 0.2 g, Temp = 25°C, pH=7.

Adsorption Thermodynamics

At the same temperature ranges of 298-318 K, the thermodynamic parameterssuch as entropy change (ΔS^0), enthalpy change (ΔH^0) and Gibbs free energy (ΔG^0) are calculated from the temperature-dependent adsorption isotherm to describe the adsorption process according to equation (7) - (9) [29]:

$$K = \frac{(C_0 - C_e)}{C_e} \quad (7)$$

$$InK_d = \frac{\Delta S^0}{R} - \frac{\Delta H^0}{RT} \quad (8)$$

$$\Delta G^0 = \Delta H^0 - T\Delta S^0 \quad (9)$$

Where C_o and C_e are the initial concentration and equilibrium concentration, R is the universal gas constant (8.314 J/mol K), and T is the absolute temperature (K). Plots of ln K versus 1/T for the adsorption of Sb (III) on Mt-HDTMA and Mt-TMPA, and the calculated values for entropy change (ΔS^0), enthalpy change (ΔH^0) and Gibbs free energy (ΔG^0) are presented in Figure 8 and Table 3 respectively. The negative values of ⊿G implies that the adsorption process is spontaneous. Also, the ⊿G value became more negative with increased temperature, demonstrating that adsorption process was more favourable at higher temperature. This explains why increase in temperature resulted in a corresponding increase in adsorption capacity (Figure 9).
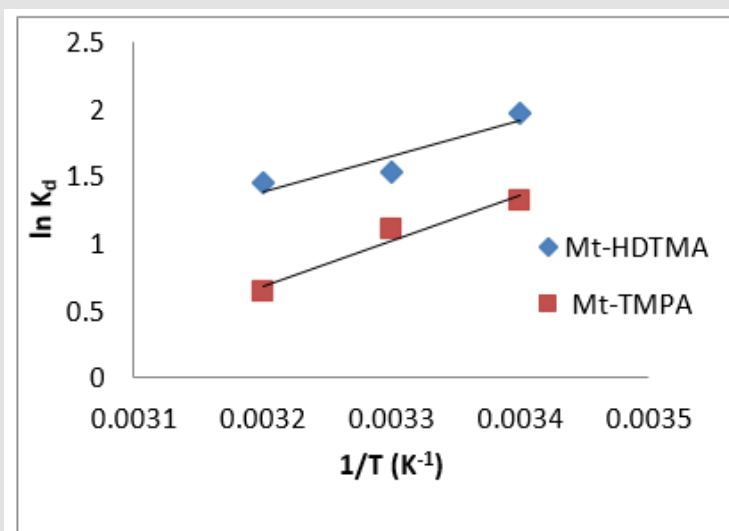
Figure 8: Plots of ln K versus 1/T for the adsorption of Sb (III) onto Mt-HDTMA and Mt-TMPA: mass of adsorbent = 0.1 g, pH=7, contact time=18 h, initial Sb (III) concentration= 50 mg/L.
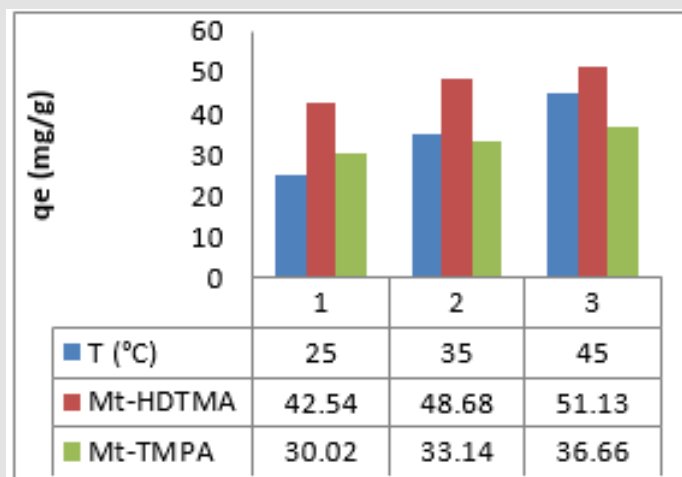
Figure 9: Effect of Temperature on the adsorption of Sb (III) by Mt-HDTMA and Mt-TMPA: Time = 18 h, Initial Sb (III) conc = 50mg/L, mass = 0.1 g, pH =7.

Table 3: Thermodynamic parameters for adsorption of Sb (lll) on Mt-HDTMA and Mt-TMPA.

ΔSo(Jmol-1K⁻¹)		ΔHo(KJmol⁻¹)	ΔGo(KJmol⁻¹)		
Adsorbent			298K	308K	318K
Mt-HDTM	57.33	32.55	-8.66	-10.9	-10.92
Mt-TMPA	62.21	19.64	-3.78	-5.18	-7.23

Again, the value of *ΔG* were not lower than -20.0 kJ·mol⁻¹, indicating that a possible surface complexation reaction was the major mechanism responsible for the adsorption [33,40-42]. The direction and magnitude of the driving force of adsorption depended on the tendency and magnitude of *ΔH*, *ΔS* and temperature [43]. Hence, the positive *ΔH* values obtained for the adsorption of Sb (III) by Mt-HDTMA and Mt-TMPA obtained as 32.55 and 19.64 kJ·mol⁻¹ indicated an endothermic adsorption [33]. The positive standard entropy changes (57.33 and 62.21 J·mol⁻¹K⁻¹ for Mt-HDTMA and Mt-TMPA respectively) indicated the increased randomness at the solid–solution interface during the adsorption of Sb (III) ions on the active sites of the organoclays [44].

Effect of pH

Solution pH is known to influence surface charge of the adsorbent and/or the adsorbate [45], which might have a great impact on the adsorption behaviour of antimony on organoclays. The adsorption capacities of Mt-HDTMA and Mt-TMPA for Sb (III) at various initial pH values ranging from 2.0 to 10 are presented in Figure 10. The adsorption capacity of Sb (III) raised from 18.3mg/g to 42.1 mg/g and 10.23 mg/g to 35.08 mg/g for Mt-HDTMA and Mt-

TMPA respectively when pH value of the initial solution increased from 2.0 to 7.0, followed by rapid reduction of adsorption capacity to 20.03 mg/g and 12.44 mg/g for Mt-HDTMA and Mt-TMPA respectively at pH of 8.0 to 10.0. Figure 10 shows that Mt-HDTMA and Mt-TMPA had a simultaneous maximum adsorption for Sb (III) when the solution was faintly acid (pH = 5.0). However maximum adsorption was attained at pH of 7. Tu, et al. [33] reported similar result. Thermal regeneration technique was applied in order to regenerate the spent organ montmorillonite at 150⁰C and at different times (2, 4, 8, 12 and 18 hrs). As seen from (Figures 11 & 12), the adsorption capacity of the regenerated organoclays were increased by increasing the regeneration time. The ratio of the sorption capacity of the regenerated adsorbent to the original adsorbent was increased from 41.28% to 95.22% for Mt-HDTMA and 30.42% to 90.46% for Mt-TMPA which corresponds to 16.57 to 38.22 mg/g and 10.14 to 30.15mg/g adsorption capacities respectively for regeneration time range of 2 to 18 hours. This result implies that HDTMA and TMPA modified montmorillonite (Mt-HDTMA, Mt-TMPA) can be repeatedly applied without any significant loss in the adsorption efficiency for Sb (III).
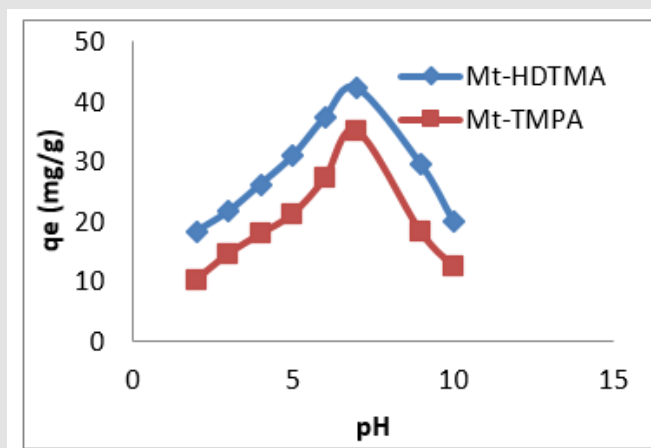
Figure 10: Effect of pH on the adsorption of Sb (III) by Mt-HDTMA and Mt-TMPA: Time = 18 h, Initial Sb (III) conc = 50 mg/L, mass = 0.1 g, Temp= 250C.
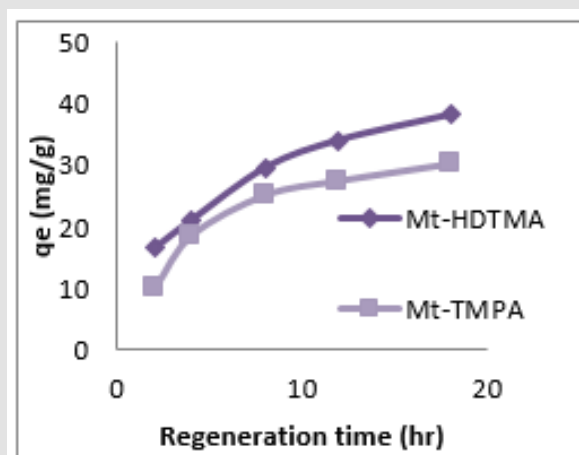
Figure 11: Effect of temperature of 1500C at various times (2 – 18 hrs) on the regeneration of Mt-HDTMA and Mt-TMPA. (Sb solution = 50 mg/L, initial pH = 7 ± 0.5, contact time = 18 hrs and mass of adsorbent = 0.2g).
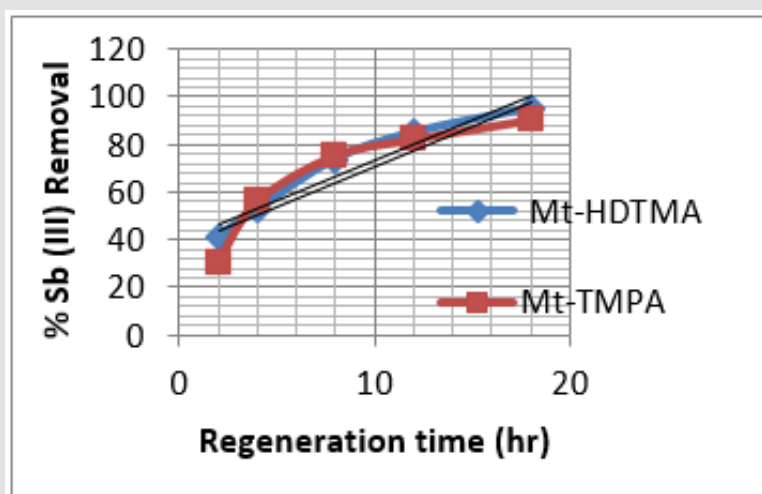
Figure 12: Percentage variation on effect of temperature of 1500C at various times (2-18hrs) on the regeneration of Mt-HDTMA and Mt-TMPA. (Sb solution = 50mg/L, initial pH = 7 ± 0.5, contact time = 18 hrs and mass of adsorbent = 0.2g).

Conclusion

The potential of HDTMA and TMPA based organoclays for effective removal of antimony Sb (III) in aqueous medium has been properly studied. Modification of organoclays enhanced effective removal of antimony in aqueous medium. Among the isotherm and kinetic model exploited, the Langmuir isotherm model and Pseudo second order kinetic model best described the sorption data. Thermodynamic studies have confirmed that the removal process of Sb (III) by both organ montmorillonite was spontaneous and endothermic. Therefore, the application of organoclays for the removal of antimony in aqueous medium via a batch adsorption process has shown promising result with auspicious future large-scale application.

Conflict of Interest

Authors declares no conflict of interest.

Funding

References

1. Targan F, Tirtom VN, Akkus B (2013) Removal of Antimony(III) from Aqueous Solution by Using Grey and Red Erzurum Clay and Application to the Gediz River Sample. Analytical Chemistry Article ID 962781.

2. Sari A, Itak DC, Tuzen M (2010) Equilibrium, thermodynamic and kinetic studies on adsorption of Sb(III) fromaqueous solution using low-cost natural diatomite. Chemical Engineering Journal 162(2): 521-527.

3. Khalid N, Ahmad S, Toheed A, Ahmed J (2000) Potential of rice husks for antimony removal, Applied Radiation and Isotopes 52(1): 31-38.

4. (1980) CEC, Council of the European Communities, Council Directive Relating to the Quality of Water Intended for Human Consumption.

5. (1984) USEPA, Antimony: An Environmental and Health Effects Assessment, US Environmental Protection Agency, Office of drinking water, Washington, DC, USA.

6. Filella M, Belzile N, Chen YW (2002) Antimony in the environment: a review focused on natural waters II. Relevant solution chemistry. Earth-Science Reviews 59(1-4): 265-285.

7. Gurnani N, Sharma A, Tulukder G (1994) Effects of antimony on cellular systems in animals: a review. Nucleus 37: 71-96.

8. Gebel T (1997) Aresnic and antimony: comparative approach on mechanistic toxicology. Chemico-Biological Interactions 107(3): 131-144.

9. Koen Oorts, Erik Smolders, Fien Degryse, Jurgen Buekers, Gabriel Gascó, et al. (2008) Solubility and toxicity of antimony trioxide (Sb_2O_3) in soil. Environmental Science and Technology 42(12): 4378-4383.

10. Smichowski P, Madrid Y, Camara C (1998) Analytical methods for antimony speciation in waters at trace and ultra trace levels. A review. Fresenius' Journal of Analytical Chemistry 360(6): 623-629.

11. Quentel F, Filella M (2002) Determination of inorganic antimony species in seawater by differential pulse anodic stripping voltammetry: stability of the trivalent state. Analytica Chimica Acta 452(2): 237-244.

12. Woolever CA, Starkey DE, Dewald HD (1999) Differential pulse anodic stripping voltammetry of lead and antimony in gunshot residues. Forensic Science International 102(31): 45-50.

13. Guin R, Das SK, Saha SK (1998) The anion exchange behaviour of Te and Sb. Journal of Radioanalytical and Nuclear Chemistry 230(1-2): 269-271.

14. Bond AM, Kratsis S, Newman OMG (1998) Combined use of differential pulse adsorptive and anodic stripping techniques for the determination of antimony (III) and antimony(V) in zinc electrolyte. Analytica Chimica Acta 372(3): 307-314.

15. Niedzielski P, Siepak M (2003) Analyticalmethods for determining arsenic, antimony and selenium in environmental samples. Polish Journal of Environmental Studies 12(6): 653-667.

16. Yu T, Zeng C, Ye M, Shao Y (2013) The adsorption of Sb(III) in aqueous solution by Fe_2O_3-modified carbon nanotubes. Water Science and Technology 68(3): 658-664.

17. Thanabalasingam P, Pickering WF (1990) Specific sorption of antimony(III) by the hydrous oxides of Mn, Fe, and Al. Water, Air and Soil Pollution 49(1-2): 175-185.

18. Hasany SM, Chaudhary MH (1996) Sorption potential of Haro River sand for removal of antimony from acidic aqueous solution. Appl Radiat Isot 47(4): 467-471.

19. Yu QM, Sun DW, Tian W, Wang GP, Shen WB, et al. (2002) Systematic studies on adsorption of trace elements Pt, Pd, Au, Se, Te, As, Hg, Sb on thiol cotton fiber. Analyt Chim Acta 456(1): 147-155.

20. Nishiyama SY, Saito K, Sugita K (2003) High-speed recovery of antimony using chelating porous hollow-fiber membrane. J Membr Sci 214(2): 275-281.

21. Bhattacharyya DK, Dutta NC (1991) Immobilization of barium, cadmium and antimony cations over zirconia. J Nucl Sci Technol 28 (11): 1014-1018.

22. Bhattacharyya DK, Dutta NC (1992) Study on the immobilization behaviour of barium, cadmium and antimony over Sn(IV) and Ce(IV) oxides. Indian J Chem Sect A 31 (2): 120-124.

23. Bagherifam S, Brown TC, Fellows CM, Naidu R, Komarneni S (2021) Highly efficient removal of antimonite (Sb (III)) from aqueous solutions by organoclay and organozeolite: Kinetics and Isotherms. Applied Clay Science 203: 106004.

24. Bagherifam S, Komarneni S, Lakzian A, Fotovat A, Khorasani R, et al. (2014a) Highly selective removal of nitrate and perchlorate by organoclay. Applied Clay Science 95: 126-132.

25. Seliem MK, Komarneni S, Parette R, Katsuki H, Cannon FS, et al. (2011) Perchlorate uptake by organosilicas, organo-clay minerals and composites of rice husk with MCM-48. Applied Clay Science 53: 621-626.

26. Schampera B, Solc R, Woche SK, Mikutta R, Dultz S, et al. (2015) Surface structure of organoclays as examined by X-ray photoelectron spectroscopy and molecular dynamics simulations. Clay Mineral 50(3): 353-367.

27. Behnsen J, Riebe B (2008) Anion selectivity of organobentonites. Applied Geochemistry 23: 2746–2752.

28. Anjum A, Datta M (2012) Adsorptive removal of antimony (III) using modified montmorillonite: a Study on Sorption Kinetics. J Analyt Sci Methods and Instrumentation 02(03): 167-175.

29. Onwuka KE, Igwe JC, Aghalibe CU, Obike AI (2020) Hexadecyltrimethyl Ammonium (HDTMA) and Trimethylphenyl Ammonium (TMPA)

Cations intercalation of Nigerian Bentonite Clay for Multi-component Adsorption of Benzene, Toluene, Ethylbenzene and Xylene (BTEX) From Aqueous Solution: Equilibrium and Kinetic Studies. Journal of Analytical Techniques and Research 2(2): 70-95.

30. Trivedi HC, Patel VM, Patel RD (1973) Adsorption of cellulose triacetate on calcium silicate, European Polymer Journal 9(6): 525-531.

31. Dixon KL, Knox AS (2012) Sequestration of Metals in Active Cap Materials: A Laboratory and Numerical Evaluation. Remediation 22(2): 81-91.

32. Onwuka KE, Emole PO, Igwe JC, Atasie OC (2022) Monitoring BTEX Adsorption onto Organoclays in Aqueous Solution: Multi-isotherm and Kinetics Studies. Biomedical Journal of Scientific and Technical Research 41: 5.

33. Tu Y, Ren L-Fei, Lin Y, Shao J, He Y, et al. (2019) Adsorption of antimonite and antimonate from aqueous solution using modified polyacrylonitrile with an ultrahigh percentage of amidoxime groups. Journal of Hazardous Materials 388: 121997.

34. Onwuka KE, Atasie OC, Emole PO, Aghalibe CU, Okafor WC (2022) Organophilicized Bentonite for Adsorptive Removal of Methylene Blue (MB) Dye in Aqueous Medium: Thermodynamics, Kinetics and Equilibrium Studies. Journal of Material Sciences & Manufacturing Research 3: 126.

35. Xi J, He M, Lin C (2011) Adsorption of antimony(III) and antimony(V) on bentonite: Kinetics, thermodynamics and anion competition. Microchem J 97(1): 85-91.

36. Salam MA, Mohamed RM (2013) Removal of antimony (III) by multi-walled carbon nanotubes from model solution and environmental samples. Chemical Engineering Research and Design 91(7): 1352-1360.

37. Leng Y, Guo W, Su S, Yi C, Xing L (2012) Removal of antimony(III) from aqueous solution by graphene as an adsorbent. Chemical Engineering Journal: 406-411.

38. Zhao X, Dou X, Mohan D, Pittman CU, Ok YS, et al. (2014) Antimonate and antimonite adsorption by a polyvinyl alcohol-stabilized granular adsorbent containing nanoscale zero-valent iron. Chemical Engineering Journal 247: 250-257.

39. Abou-Mesalam MM (2004) Applications of inorganic ion exchangers: II-Adsorption of some heavy metal ions from their aqueous waste solution using synthetic Iron (III) Titanate. Adsorption 10: 87-92.

40. Siyal AA, Shamsuddin MR, Khan MI, Rabat NE, Zulfiqar M, et al. (2018) A review on geopolymers as emerging materials for the adsorption of heavy metals and dyes. Journal of Environmental Management 224: 327-339.

41. Wang CC, Chang CY, Chen CY (2001) Study on Metal Ion Adsorption of Bifunctional Chelating Ion- Exchange Resins. Macromolecular Chemistry & Physics 202(6): 882-890.

42. Li L, Liu F, Jing X, Ling P, Li A (2011) Displacement mechanism of binary competitive adsorption for aqueous divalent metal ions onto a novel IDA-chelating resin: Isotherm and kinetic modeling. Water Research 45(3): 1177-1188.

43. Yang X, Zhou S, Yuan M, Liu L (2015) Adsorption of Trivalent Antimony from Aqueous Solution Using Graphene Oxide: Kinetic and Thermodynamic Studies. Journal of Chemical & Engineering Data 60(3): 806-813.

44. Bode-Aluko CA, Pereao O, Ndayambaje G, Petrik L (2016) Adsorption of Toxic Metals on Modified Polyacrylonitrile Nanofibres: A Review. Water, Air, & Soil Pollution 228(1): 35-45.

45. Luo J, Luo X, Crittenden J, Qu J, Bai Y, et al. (2015) Removal of Antimonite (Sb (III)) and Antimonate (Sb(V)) from Aqueous Solution Using Carbon Nanofibers That Are Decorated with Zirconium Oxide (ZrO_2). Environmental Science & Technology 49(18): 11115-11124.

Assets of Publishing with us

- Global archiving of articles
- Immediate, unrestricted online access
- Rigorous Peer Review Process
- Authors Retain Copyrights
- Unique DOI for all articles

https://biomedres.us/